ResearchGate

See discussions, stats, and author profiles for this publication at: https://www.researchgate.net/publication/225018874

Cyclic Delay Diversity: Effective Channel Properties and Applications

Conference Paper · October 2006

Source: DLR

CITATIONS
13

READS
1,235

2 authors:

Armin Dammann
German Aerospace Center (DLR)
284 PUBLICATIONS **2,546** CITATIONS

SEE PROFILE

Simon Plass
German Aerospace Center (DLR)
110 PUBLICATIONS **893** CITATIONS

SEE PROFILE

All content following this page was uploaded by Simon Plass on 22 June 2014.

The user has requested enhancement of the downloaded file.

Comcast, Ex. 1017

Cyclic Delay Diversity: Effective Channel Properties and Applications

Armin Dammann and Simon Plass, *Member, IEEE*

***Abstract*— We briefly explain the concept of cyclic delay diversity (CDD) as a variant of standard conformable delay diversity techniques. Usually being implemented at the transmitter side of an OFDM based system, the application of CDD is recognized at the receiver side only by observing modified channel propagation conditions. Therefore, we analyze the effect of CDD on the channel fading properties observed by a receiver in terms of the effective channel transfer function and the effective subcarrier fading correlation function. These modified properties provide the possibility for optimizing diversity and coding gain of mobile radio communications systems. Simulations show the performance improvement capabilities of CDD for the terrestrial digital video broadcasting system (DVB-T) and to a cellular mobile radio communications system.**

***Index Terms*— Cyclic Delay Diversity (CDD), Cellular Cyclic Delay Diversity (C-CDD), DVB-T, OFDM**

I. Introduction

Recently, multiple-antenna concepts have become popular, since they offer higher spectral efficiency, and therefore, increase the achievable data throughput in wireless communications systems. Tarokh et.al. [1] proposed a multiple antenna concept called Space-Time coding, which provides and exploits diversity based on trellis codes. The well-known Alamouti scheme [2] is a representative of Space-Time block codes. However, the idea of increasing diversity by using multiple transmit (TX) antennas was not new at that time. In [3] and [4], for example, TX-antenna specific signal modifications, *i.e.* additional signal delays and Doppler shifts, have already been identified as sources of diversity. In [5]–[7], these ideas were adopted to wireless communications systems using cyclic extensions as guard intervals — in particular OFDM systems — with the concept of *cyclic delay diversity (CDD)* as a variant of *delay diversity (DD)*. One advantage of those schemes is their standard compatibility. This means, that a receiver does not necessarily have to be aware of their implementation at the transmitter side. A receiver will therefore observe modified channel propagation conditions when CDD is implemented in addition. In this paper we focus on CDD and analyze its influence on the channel propagation properties in terms of the effective channel transfer function and subcarrier fading correlation. Together with channel- and/or spreading-code properties the effective subcarrier fading process correlation provides a possibility to increase resp. optimize the system performance of wireless communications systems by a systematic design of the CDD parameters [8]. Exemplarily, we apply CDD to the terrestrial digital video broadcasting system (DVB-T) and to a cellular mobile radio communications system, based on orthogonal frequency division multiple access (OFDMA),

A. Dammann and S. Plass are with the Institute of Communications and Navigation, German Aerospace Center (DLR), Oberpfaffenhofen, 82234 Wessling, Germany, Email: {Armin.Dammann, Simon.Plass}@DLR.de

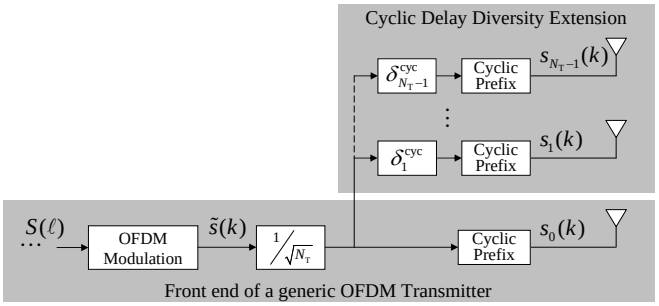

Fig. 1. Principle of cyclic delay diversity

and show the performance improvement capabilities by simulations.

II. Cyclic Delay Diversity

In this section, we briefly introduce CDD. In principle, CDD shifts the TX-signal in time direction and transmit these modified signal copies over separate TX-antennas. The TX-antenna specific signal modifications, *i.e.* the time shifts, are inserted in cyclically, such that no additional inter symbol interference (ISI) occurs. CDD is capable to offer a larger degree of diversity since they increase the number of resolvable channel propagation paths. This additional diversity has to be exploited by the OFDM system itself by means of techniques, which guarantee a certain amount of Hamming distance for the data bearing signal, *i.e.* channel coding or spreading.

Fig. 1 shows the front end of a CDD OFDM transmitter. For simplicity of the notation, we consider the transmission of one OFDM symbol. N data symbols $S(\ell),\ \ell = 0,\ldots,N-1$ are obtained from a precedent coding, modulation, and framing part. These complex valued symbols are transformed into time domain by the OFDM entity using an inverse fast Fourier transform (IFFT). This results in N time domain samples $\tilde{s}(k),\ k = 0,\ldots,N-1$. Before inserting a cyclic prefix as guard interval, the time domain OFDM symbol is shifted cyclically by δ_i^{cyc} in each TX antenna branch. This yields the antenna specific TX-signals

$$s_i(k) = \frac{1}{\sqrt{N_{\text{T}}}} \cdot \tilde{s}(k - \delta_i^{\text{cyc}} \bmod N), \quad i = 0,\ldots,N_{\text{T}}-1, \tag{1}$$

where N_{T} is the number of TX-antennas. Without loosing generality, we transmit the unshifted signal over TX-antenna 0, *i.e.*, $\delta_0^{\text{cyc}} = 0$. The time domain signal including the guard interval is obtained for $k = -N_{\text{G}},\ldots,N-1$, where N_{G} is the guard interval length. In contrast to cyclic shifts δ_i^{cyc} in case of CDD, simple delay diversity (DD) just shifts the original data signal in time domain by TX-antenna specific delays δ_i. Both CDD and DD yield the same signal at the receiver after guard interval removal as long as $\delta_i =$

$\delta_i^{\mathrm{cyc}},\ i = 0, \ldots, N_{\mathrm{T}} - 1$ and the received signal is free of ISI. To avoid ISI, the guard interval length N_{G} in samples has to fulfill

$$N_{\mathrm{G}} \geq \begin{cases} N_{\max} + \max_i \delta_i, & \text{for DD} \\ N_{\max}, & \text{for CDD,} \end{cases} \quad (2)$$

where $N_{\max}$ denotes the maximum channel delay in samples. The minimum length of the guard interval for CDD does not depend on the cyclic delays δ_i^{cyc}, which allows shorter guard intervals compared to DD.

III. Influence on the Channel Properties

In this section, we analyze CDD in terms of the effective channel transfer function and subcarrier fading correlation. The received time domain signal is the superposition of the N_{T} TX signals in (1)

$$r(k) = \frac{1}{\sqrt{N_{\mathrm{T}}}} \sum_{i=0}^{N_{\mathrm{T}}-1} \sum_{p=0}^{N_{\max}} s(k - p - \delta_i^{\mathrm{cyc}} \bmod N) \cdot h_i(k,p) \quad (3)$$

for $k = 0, \ldots, N-1$. $h_i(k,p)$ denotes the time domain fading process (time index is k) for TX-antenna i and path delay p (in samples). The factor $\frac{1}{\sqrt{N_{\mathrm{T}}}}$ normalizes the average transmitted signal power to one. Since we are interested in the effective channel transfer function and subcarrier fading correlation, we neglect additive white Gaussian noise (AWGN).

We transform the received time domain signal into the frequency domain and get

$$\begin{aligned} R(\ell) &= \frac{1}{\sqrt{N}} \sum_{k=0}^{N-1} r(k) \cdot e^{-j\frac{2\pi}{N}\cdot k \cdot \ell} \\ &= \frac{1}{\sqrt{N \cdot N_{\mathrm{T}}}} \sum_{\nu=0}^{N} S(\nu) \cdot \\ &\sum_{i=0}^{N_{\mathrm{T}}-1} \sum_{p=0}^{N_{\max}} H_i(\ell - \nu \bmod N, p) \cdot e^{-j\frac{2\pi}{N}\cdot(p+\delta_i^{\mathrm{cyc}})\cdot\nu}, \end{aligned} \quad (4)$$

where

$$H_i(q,p) = \frac{1}{\sqrt{N}} \sum_{k=0}^{N-1} h_i(k,p) \cdot e^{-j\frac{2\pi}{N}\cdot k \cdot q} \quad (5)$$

is the discrete Fourier transform (DFT) of length N of the time variant channel fading process $h_i(k,\ell)$ with respect to time index k. $S(q)$ denotes the DFT of $s(k)$. From (4) we can observe the following:

- The effects of CDD can be assigned to the channel, i.e. we observe a modified or transferred channel at the receiver.
- Due to the convolution in frequency domain (expressed by $\sum_{q=0}^{N} \ldots$ in (4)) we get intercarrier interference (ICI) in general. This simplifies to the well known parallel (ICI-free) transmission over subcarriers if the fading processes $h_i(k,p) = \text{const.} = h_i(p)$ are constant for the duration of an OFDM symbol.

In case of quasi static fading (4) simplifies to

$$R(\ell) = S(\ell) \cdot \frac{1}{\sqrt{N_{\mathrm{T}}}} \cdot \sum_{i=0}^{N_{\mathrm{T}}-1} e^{-j\frac{2\pi}{N}\cdot\delta_i^{\mathrm{cyc}}\cdot\ell} \cdot \underbrace{\sum_{p=0}^{N_{\max}} h_i(p) \cdot e^{-j\frac{2\pi}{N}\cdot p\cdot\ell}}_{=\sqrt{N}\cdot H_i(\ell)} \quad (6)$$

A. Channel Transfer Function

With the quasi static channel fading assumption we have got the well known description of OFDM in frequency domain, where each transmitted data symbol is multiplied by a complex valued fading coefficient when observed at the receiver. Thus, we can rewrite (6) as $R(\ell) = S(\ell) \cdot \tilde{H}(\ell)$ with the equivalent channel transfer function

$$\tilde{H}(\ell) = \sqrt{\frac{N}{N_{\mathrm{T}}}} \sum_{i=0}^{N_{\mathrm{T}}-1} \cdot H_i(\ell) \cdot e^{-j\frac{2\pi}{N}\cdot\delta_i^{\mathrm{cyc}}\cdot\ell}, \quad (7)$$

which comprises the CDD implementation effects. $H_i(\ell)$ are the frequency domain channel fading coefficients for subcarrier ℓ of the transmitted OFDM symbol from TX-antenna i to the receiver. Be careful not to mix $H_i(\ell)$ up with $H_i(q,p)$ as defined in (5). The first one is the DFT of $h_i(k,p)$ with respect to the path delay p and the quasi-static fading assumption (*i.e.* $h_i(k,p) = h_i(p)$). The latter is the DFT of $h_i(k,p)$ with respect to the time variable k and path delay p as a parameter.

B. Fading Correlation

In the following we are interested in the correlation of the frequency domain channel fading processes $\tilde{H}(\ell)$ in frequency direction. The expectation $E\{\tilde{H}^*(\ell)\cdot\tilde{H}(\ell+\nu \bmod N)\}$ yields the correlation properties of the frequency domain channel fading, where $(\cdot)^*$ means complex conjugate. We assume complex valued zero mean stochastic processes $h_i(p)$, which are independently distributed with respect to the path delay p and TX-antenna i. Furthermore, these processes shall be stationary. Since we assume identical statistical channel properties from TX-antenna i to the receiver, σ_p does not depend on TX-antenna index i. With these properties, the fading correlation in frequency direction is

$$\begin{aligned} \Phi(\nu) &= E\{\tilde{H}^*(\ell) \cdot \tilde{H}(\ell + \nu \bmod N)\} \\ &= \underbrace{\frac{1}{N_{\mathrm{T}}} \sum_{i=0}^{N_{\mathrm{T}}-1} e^{-j\frac{2\pi}{N}\cdot\delta_i^{\mathrm{cyc}}\cdot\nu}}_{\triangleq\Phi^{\mathrm{CDD}}(\nu)} \cdot \underbrace{\sum_{p=0}^{N-1} \sigma_p^2 \cdot e^{-j\frac{2\pi}{N}\cdot p\cdot\nu}}_{\triangleq\Phi^{\mathrm{Ch}}(\nu)}, \end{aligned} \quad (8)$$

where $\sigma_p^2 = E\{|h_i(p)|^2\}$. $\Phi^{\mathrm{Ch}}(\nu)$ is the fading correlation function in frequency direction for the component channels, *i.e.* the channel observed from each TX-antenna i to the receiver antenna. We observe from (8) that the channel and CDD influence are separated factors. This is an important property and allows the design of roots for the correlation function ($\Phi(\nu) = 0$) for dedicated values ν independent of the multipath channel properties $\Phi^{\mathrm{Ch}}(\nu)$.

C. Choice of δ_i^{cyc}

If the TX-antenna specific cyclic delays δ_i^{cyc} are increasing with a constant increment of δ, *i.e.* they are chosen as

$$\delta_i^{\mathrm{cyc}} = \delta \cdot i, \quad i = 0, \ldots, N_{\mathrm{T}} - 1 \tag{9}$$

we get

$$\Phi^{\mathrm{CDD}}(\nu) = \frac{1}{N_{\mathrm{T}}} \cdot e^{-j\frac{\pi\delta(N_{\mathrm{T}}-1)}{N}\cdot\nu} \cdot \frac{\sin\left(\frac{\pi\delta N_{\mathrm{T}}}{N}\cdot\nu\right)}{\sin\left(\frac{\pi\delta}{N}\cdot\nu\right)}. \tag{10}$$

We consider 2 cases:

i) N_{T} is a divider of N:
We set $\delta = \frac{N}{N_{\mathrm{T}}}$ and (10) simplifies to

$$\Phi^{\mathrm{CDD}}(\nu) = \delta(\nu \bmod N_{\mathrm{T}}). \tag{11}$$

Considering a specific subcarrier, this means that a subcarrier fading process is uncorrelated to its $N_{\mathrm{T}} - 1$ neighbors.

ii) We choose δ such that $\delta \cdot N_{\mathrm{T}}$ is a divider of N:
With $\eta = \frac{N}{\delta \cdot N_{\mathrm{T}}}$

$$\Phi^{\mathrm{CDD}}(\nu) = \frac{1}{N_{\mathrm{T}}} \cdot e^{-j\frac{\pi(N_{\mathrm{T}}-1)}{\eta\cdot N_{\mathrm{T}}}\cdot\nu} \cdot \frac{\sin\left(\frac{\pi}{\eta}\cdot\nu\right)}{\sin\left(\frac{\pi\cdot\nu}{\eta\cdot N_{\mathrm{T}}}\right)}. \tag{12}$$

This choice yields decorrelation of subcarriers in intervals of η. In intervals of $\eta \cdot N_{\mathrm{T}}$, however, we observe full correlation, *i.e.* $\Phi^{\mathrm{CDD}}(\eta N_{\mathrm{T}} \cdot i) = 1$.

As already mentioned, the systematic designable correlation properties of the subcarrier fading processes can be used for optimizing diversity and coding gain exploited by channel- or spreading-codes [8]. Thus, it is possible to approach or even reach independent Rayleigh fading propagation performance, which is the optimum in terms of diversity for non line-of-sight propagation.

IV. Applications

A. Terrestrial Digital Video Broadcasting (DVB-T)

In many countries, terrestrial digital video broadcasting system (DVB-T) [9] is currently replacing analogue TV broadcasting systems. The digital technology offers more channels in the same bandwidth together with additional services and higher quality.

1) System Description: Fig. 2 shows the principle physical layer block diagram for a DVB-T transmitter including a CDD front end extension in the base band. This system can be separated in 3 major parts:

i) MPEG-2 source coding and multiplexing
ii) Outer Reed-Solomon channel coding and (convolutional) interleaving ("outer coding" part)
iii) Inner convolutional channel coding, interleaving and QAM modulation ("inner system" part)

DVB-T is able to provide hierarchical coding and modulation with two levels, which results in unequal error protection for two different bit streams. Fig. 2 shows this property by means of two coding and interleaving branches. For the outer part, the DVB-T standard specifies a shortened Reed-Solomon code of length 204 and dimension 188. The code symbols (bytes) of this code are elements of the binary extension field $\mathrm{GF}(2^8)$ [9]. The cardinality of this field provides the length of the Reed-Solomon mother code as $2^8 - 1 = 255$. The inner system part includes a $(171, 133)_{\mathrm{oct}}$ convolutional code of memory 6 and code rate 1/2. Higher code rates are achieved by puncturing.

TABLE I
Power-delay profiles of simulation channel models

(a) Indoor Commercial – Channel B

Tap	Rel. delay [ns]	Rel. power [dB]
1	0	−4.6
2	50	0
3	150	−4.3
4	225	−6.5
5	400	−3.0
6	525	−15.2
7	750	−21.7

(b) Outdoor Residential – High Antenna – Channel B

Tap	Rel. delay [ns]	Rel. power [dB]
1	0	−6.0
2	450	−3
3	500	0
4	1050	−1.5
5	3250	−4.7
6	6000	−3.0
7	8300	−12.0
8	10000	−14.5
9	12050	−17.4
10	15000	−21.7

TABLE II
Mobile velocities and Doppler bandwidths for a carrier frequency of 1 GHz

	Indoor	Outdoor
Carrier frequency	1 GHz	
Doppler bandwidth	10 Hz	50 Hz
Spectrum form	rectangular	Jakes
Mobile velocity	10.8 km/h (3 m/s)	54 km/h (15 m/s)

Fig. 3 shows exemplarily the receiver block diagram for 2 RX-antennas. Guard interval removal and OFDM demodulation is performed separately in each RX-antenna branch. The received symbols are combined using subcarrier-wise maximum ratio combining (MRC). Subsequent QAM demodulation provides log-likelihood ratios as soft input for the inner channel decoder, which is a soft-decision Viterbi decoding algorithm for the inner convolutional code. For our investigations, we focus on the inner system. This means we measure the bit error rate (BER) at the output of the (inner) Viterbi decoder. In [9] the target BER at that point is specified as $2 \cdot 10^{-4}$. This results in a quasi error free data stream after the outer Reed-Solomon decoder. The respective data stream at the transmitter side, *i.e.* the convolutional encoder input, is modeled as statistically independent random bit stream.

2) Channel Models: For simulations, we use multipath Rayleigh fading channel models with non line-of-sight (NLOS) propagation. A detailed specification of these models can be found in [10]. The power-delay profiles for the *indoor commercial* and the *outdoor residential – high antenna* models are shown in Table I. It can be seen, that the indoor scenario shows a smaller delay spread compared to the outdoor environment. We do not consider a path loss model and restrict to the so-called *B-type* channels of that specification, which show a medium delay spread relative to the considered scenario. Table II shows the Doppler characteristics for the simulations.

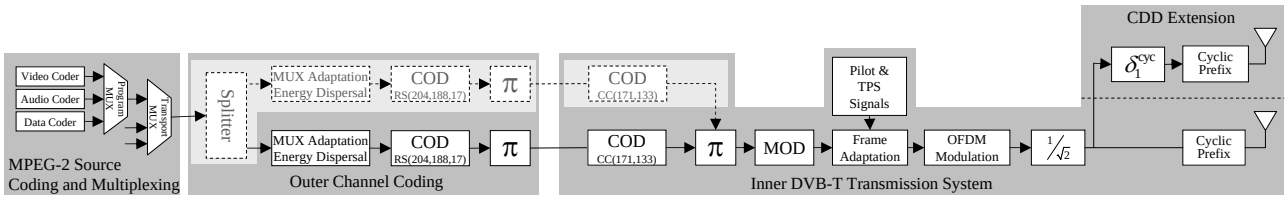

Fig. 2. Physical layer of DVB-T transmitter with CDD

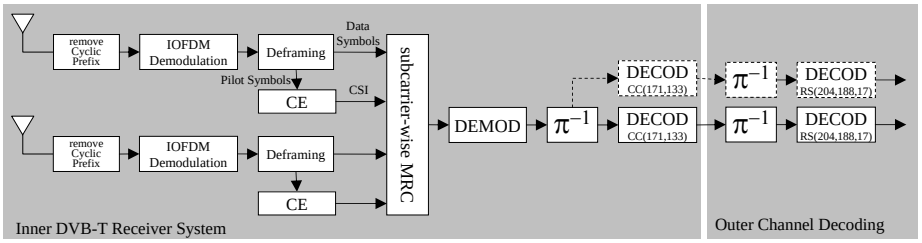

Fig. 3. Inner physical layer of a DVB-T diversity receiver

According to the specification in [10], the indoor model is dedicated for large open centers, such as shopping malls and airports, whereas the outdoor model covers scenarios with single and double store buildings aside roads having two lanes and cars parked along the street sides.

3) Simulation Results: We consider both a single-TX and a 2-TX antenna CDD DVB-T transmitter. The overall transmitted power is normalized to the number of TX antennas. At the receiver side, we use a standard single-RX antenna front-end and compare its performance with that of a 2-RX antenna MRC receiver. Subsequently, the BER results are plotted versus E_S/N_0, which denotes the average received signal power per data subcarrier and RX antenna divided by the variance of the complex valued Gaussian noise. This means, we do not normalize the received signal power to the number of RX antennas and do not consider the code rate and guard interval length for SNR (E_S/N_0) calculation. SNR differences among BER graphs are in general specified for a BER $= 2 \cdot 10^{-4}$. This BER causes a quasi error free transmission after decoding of the outer Reed-Solomon code.

Fig. 4 and Fig. 5 shows the BER vs. E_S/N_0 for both the indoor and outdoor propagation scenario. The DVB-T system operates in the 2k mode ($N = 2048$) using 4-QAM modulation and a code rate of $R = 1/2$. The BER performance of the respective 1-TX-antenna systems are plotted as references. Applying 2-TX-antenna CDD at the transmitter with a cyclic delay of $\delta_1^{\mathrm{cyc}} = 10$ samples, which equals 1.1 μs, yields an SNR gain of 3.3 dB for the indoor channel and 1.4 dB for the outdoor channel. The additional diversity, provided by the transmitter, is exploited by the channel code at the receiver. Using a 1-TX/2-RX-antenna MRC receiver results in a performance improvement of approximately 6 dB for both channels. This gain consists of a receiver SNR gain of 3 dB due to coherent subcarrier-wise superposition and a diversity gain, which is provided by MRC in combination with the channel code. An additional application of 2-TX CDD at the transmitter yields a further improvement of 1.75 dB in the indoor case and 0.8 dB in the outdoor case compared to the 1-TX/2-RX system.

Fig. 6 shows the SNR gain for CDD with different cyclic delay using single-antenna and 2-antenna MRC receivers. It can be observed, that there is a saturation effect, *i.e.*a cyclic delay of $\delta_1^{\mathrm{cyc}} > 1.5$ μs results in no further improvement.

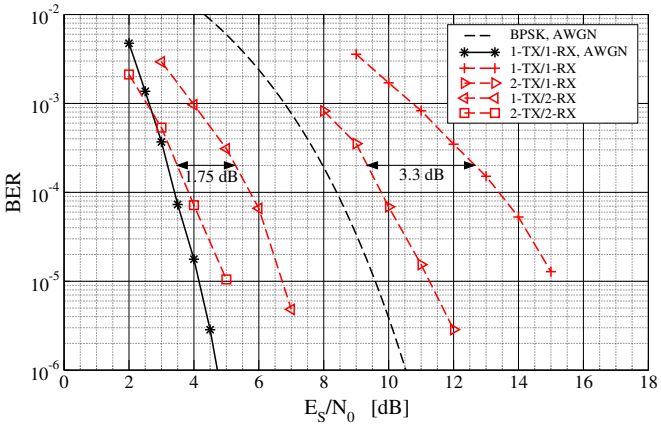

Fig. 4. BER vs. E_S/N_0; $\delta_1^{\mathrm{cyc}} = 10$ samples ($\approx$ 1.1 μs) for 2-TX antenna systems; indoor channel

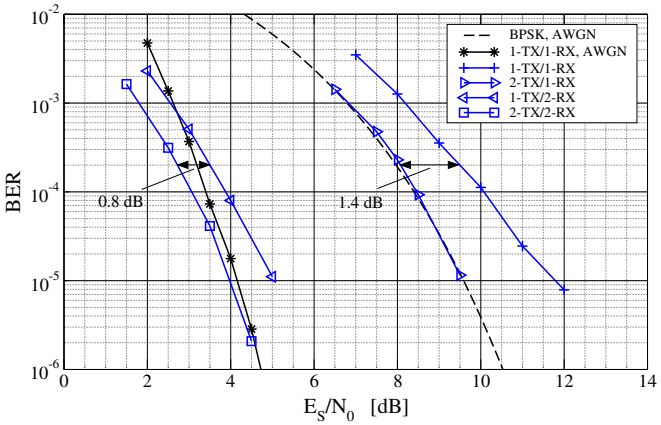

Fig. 5. BER vs. E_S/N_0; $\delta_1^{\mathrm{cyc}} = 10$ samples ($\approx$ 1.1 μs) for 2-TX antenna systems; outdoor channel

Different from the indoor results, the outdoor delay diversity gain shows local minima for $\delta_1^{\mathrm{cyc}} \approx 0.55$ μs. In that case, powerful propagation paths of the outdoor channel model overlap (cf. the power-delay profile, shown in Table I(b)). In particular, these are tap 4 (1050 ns, -1.5 dB) and tap 3 (500 ns, 0 dB), which — together with the cyclic delay of $\delta_1^{\mathrm{cyc}} \approx 0.55$ μs — also results in an effective delay of 1050 ns.

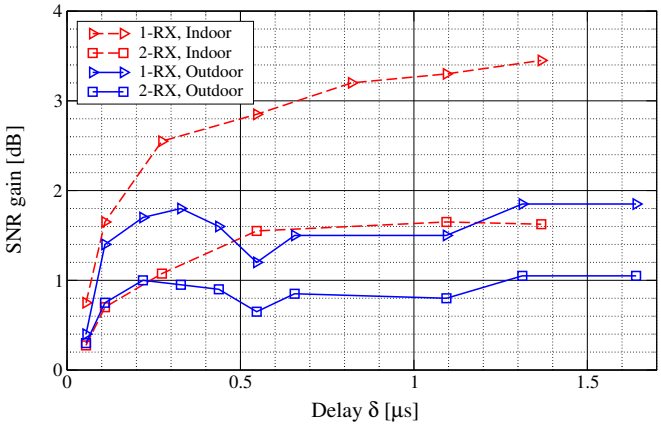

Fig. 6. SNR gain vs. cyclic delay δ_1^{cyc} of 2-TX antenna CDD compared to the respective 1-TX antenna system at $\mathrm{BER} = 2 \cdot 10^{-4}$

B. Cellular Mobile Radio Communications Systems

1) Cellular Environment: We consider a synchronized cellular system in time and frequency with two cells, see Fig. 7. The kth BS has a distance d_k to the desired MT. The superimposed signal at the MT is given by

$$R(l) = S^{(0)}(l)H^{(0)}(l) + S^{(1)}(l)H^{(1)}(l) + N(l)\,. \qquad (13)$$

The signal energy attenuation due to path loss is generally modeled as the product of the γth power of distance d_k. γ represents the path loss factor. Depending on the position of the MT the carrier-to-interference ratio (C/I) varies and is defined by

$$\frac{C}{I} = \frac{E\{|S^{(0)}(l)H^{(0)}(l)|^2\}}{E\{|S^{(1)}(l)H^{(1)}(l)|^2\}} \cdot \left(\frac{d_0}{d_1}\right)^{-\gamma}. \qquad (14)$$

For geometrical simplification, we assume that the position of the MT terminal is located on the direct line between the two BSs.

2) Channel Model: The channel model C of the IEEE 802.11n standard is chosen in this paper. This model represents a large open space (indoor and outdoor) with non-line-of-sight conditions of a short range scenario. Therefore, the maximum cell size is chosen to $r = 300$ m. The channel is modeled by a tapped delay-line model with 14 taps and a maximum delay $\tau_{\max} = 200$ ns. In this environment the path loss is defined by $\gamma = 3.5$ [11]. This channel model and propagation model are used throughout all cells.

3) Cellular Cyclic Delay Diversity: At the cell border of a conventional OFDMA system, inter-cellular interference exists, and therefore, the used subcarrier resources are underachieved. On the other hand, the avoidance of interference does not allow double allocation of subcarriers from adjacent BSs. This decreases the exploitation of the subcarrier resources per BS. Cell sectorization could ease this problem to two BSs. The CDD principle can be applied in a cellular environment by using adjacent BSs. This leads to the new *cellular cyclic delay diversity (C-CDD)* scheme. C-CDD takes advantage of the aforementioned resulting available resources. The main goal is to increase performance by avoiding interference and increasing diversity at the most critical environment.

For C-CDD the interfering BS also transmits a copy of the victim's signal as the desired BS to the designated MT located in the broadcast area. Additionally, a cyclic shift is

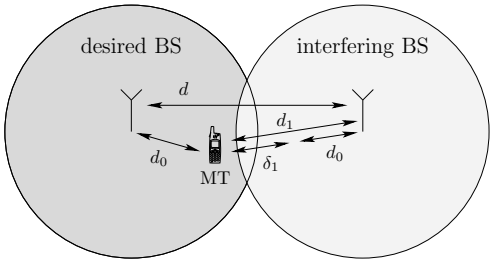

Fig. 7. Cellular environment

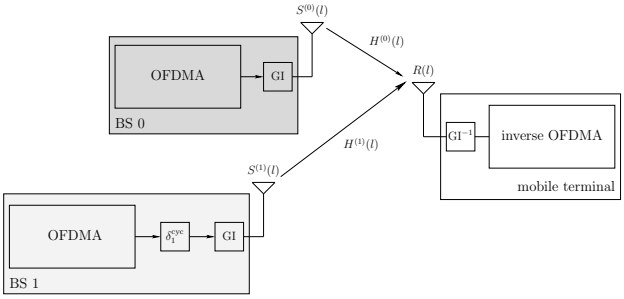

Fig. 8. Cellular OFDMA system with cellular cyclic delay diversity (C-CDD)

inserted to this signal, see Fig. 8 and at the MT the received signal can be described by

$$R(l) = S^{(0)}(l)(H^{(0)}(l) + H^{(1)}(l)e^{-j\frac{2\pi}{N_{\mathrm{FFT}}}\delta_1^{\mathrm{cyc}} \cdot l})\,. \qquad (15)$$

The transmission of the signal is synchronous in the cellular system and the delays of the received OFDMA signal nearby the cell border are smaller than the guard interval. Furthermore, at the MT the superimposed statistically independent Rayleigh distributed channel coefficients from the different BSs sum up again in a Rayleigh distributed channel coefficient. The usage of cyclic shifts prevents the occurrence of additional ISI. For C-CDD no additional configurations at the MT for exploiting the increased transmit diversity are necessary.

On the other side, for the C-CDD concept each involved BS has to transmit additionally the signal of the adjacent cell, and therefore, a higher amount of resources are allocated at each BS.

Finally, the C-CDD technique inherently provides another transmit diversity technique. If no cyclic shift δ_k^{cyc} is introduced, the signals from the different BSs may arrive at the desired MT with different delays δ_k. These delays can be also seen as delay diversity (DD) [4] for the transmitted OFDMA signal. Therefore, an inherent transmit diversity, namely cellular delay diversity (C-DD), is introduced if the adjacent BSs just transmit the same desired signal at the same time to the designated MT.

In our scenario with two BSs, the distances of the BSs to the MT correspond directly to the delay $\delta_1 = d - 2d_0$ due to Fig. 7. Furthermore, the transmitted data in each cell is limited to a maximal resource load of 0.5. Since the transmitted energy at each BS is the same, $E\{|S_i^{(0)}|^2\} = E\{|S_i^{(1)}|^2\}$, and therefore using (14),

$$C/I = \left(\frac{d_0}{d - d_0}\right)^{-\gamma}, \qquad \delta_1 = d - \left(\frac{2d}{\sqrt[\gamma]{C/I} + 1}\right). \qquad (16)$$

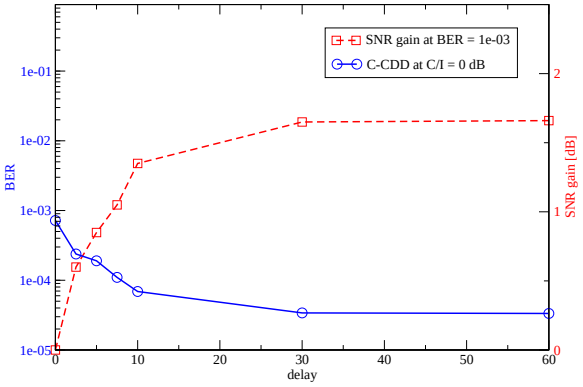

Fig. 9. BER and SNR gain versus the cyclic delay at the cell border ($\mathrm{C/I} = 0$ dB)

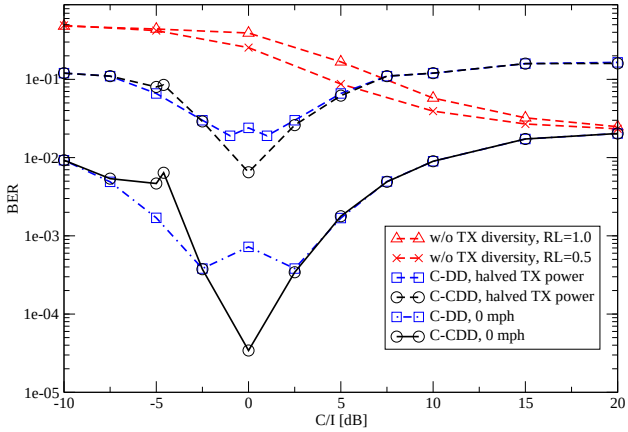

Fig. 10. BER versus C/I for 4-QAM using no transmit diversity technique, C-DD, and C-CDD

Both δ_1 and C/I depend on the MT distance d_0. This provides a relation between δ_1 and C/I. The overall delay in the cellular system can be expressed by

$$\delta = \delta_1 + \delta_1^{\mathrm{cyc}} \,. \tag{17}$$

For C-CDD the term C/I (cf. (14)) may be misleading, as there is no I (interference). On the other hand it describes the ratio of the power from the desired base station to the temporary BS and indicates where the MT is in respect to the BSs.

Radio resource management works perfectly if all information about the mobile users, like the channel state information, is available at the base station. This is especially true if the RRM could be intelligently managed by a single genie manager. As this will be very unlikely, the described scheme offers an improved performance especially at the critical cell border without the need of any information about the channel state information on the transmitter side.

4) Simulation Results: The simulation environment is based on the parameter assumptions of the IST-project WINNER for next generation mobile communications system [12]. The used channel model is the 14 taps IEEE 802.11n channel model C with $\gamma = 3.5$. The transmission system is based on a carrier frequency of 5 GHz, a bandwidth of 100 MHz, and an FFT length of $N_{\mathrm{c}} = 2048$. One OFDM symbol length (excluding the GI) is $20.48\ \mu$s and the GI is set to $0.8\ \mu$s (corresponding to 80 samples). For the simulations, 4-QAM or 16-QAM is used, the SNR is set to 5 dB, and perfect channel knowledge is assumed. Furthermore, a $(561, 753)_{\mathrm{oct}}$ convolutional code with rate $R = 1/2$ was selected as channel code. We assume statistically independent channels with equal stochastic properties from each BS to the MT.

Fig. 9 shows the influence of the cyclic delay δ_1^{cyc} to the BER and the SNR gain at the cell border ($C/I = 0$ dB) for C-CDD. At the cell border there is no influence due to C-DD, *i.e.*, ($\delta_1 = 0$). Two characteristics of the performance can be highlighted. First, there is a performance loss for $\delta_1^{\mathrm{cyc}} = 0$ due to the missing C-CDD. Secondly, the best performance can be achieved for an existing higher cyclic shift which reflects the results in [13]. The SNR gain performance for a target BER of 10^{-3} depicts also the influence of the increased cyclic delay. For higher delays the performance saturates at a gain of 1.7 dB.

The performances of the applied C-DD and C-CDD methods are compared in Fig. 10 with the reference system using no transmit diversity technique for 4-QAM. The reference system is half ($\mathrm{RL} = 0.5$) and fully loaded ($\mathrm{RL} = 1.0$). We observe a large performance gain in the close-by area of the cell border ($C/I = -10$ dB$\ldots 10$ dB) for the new proposed diversity techniques C-DD and C-CDD. Furthermore, C-CDD enables an additional substantial performances gain at the cell border. The C-DD performance degrades for $C/I = 0$ dB because $\delta = 0$ and no transmit diversity is available. The same effect can be seen for C-CDD at $C/I = -4.6$ dB ($\delta_1 = -30$, $\delta_1^{\mathrm{cyc}} = 30 \Rightarrow \delta = 0$). Since both BSs in C-DD and C-CDD transmit the signal with the same power as the single BS in the reference system, the received signal power at the MT is doubled. Therefore, the BER performance of C-DD and C-CDD at $\delta = 0$ is still better than the reference system performance. For higher C/I ratios, *i.e.*in the inner cell, the C-DD and C-CDD transmit techniques lack the diversity from the other BS, and therefore, the performances merge to the reference performances. To establish a more detailed understanding we analyze the C-CDD with halved transmit power. For this scenario, the total designated received power at the MT is equal to the conventional OFDMA system. There is still a performance gain due to the exploited transmit diversity for $C/I < 5$ dB. The performance characteristics are the same for halved and full transmit power. C-DD at $C/I = 0$ dB also represents the conventional OFDMA single-user case without any inter-cellular interference. Another benefit of the halved transmit power for the used C-CDD subcarriers is a reduction of the inter-cellular interference for the neighboring cells.

Since we assume the total number of subcarriers is equally distributed to the maximum number of users per cell, each user has a maximum throughput of $\eta_{\max}$. We regard the maximum throughput of 16-QAM as the reference value for $\eta_{\max}$. Therefore, the maximum throughput of the 4-QAM systems is $\eta_{\max}/2$. The throughput η of the system, by using the probability $P(n)$ of the first correct OFDM frame transmission after $n-1$ failed retransmissions, is given by

$$\eta = \sum_{n=0}^{\infty} \frac{\eta_{\max}}{n+1} P(n) \geq \eta_{\max}(1 - FER) \,. \tag{18}$$

A lower bound of the system is given by the right hand side of (18) by only considering $n = 0$ and the frame error rate (FER). Fig. 11 illustrates this lower bound for different

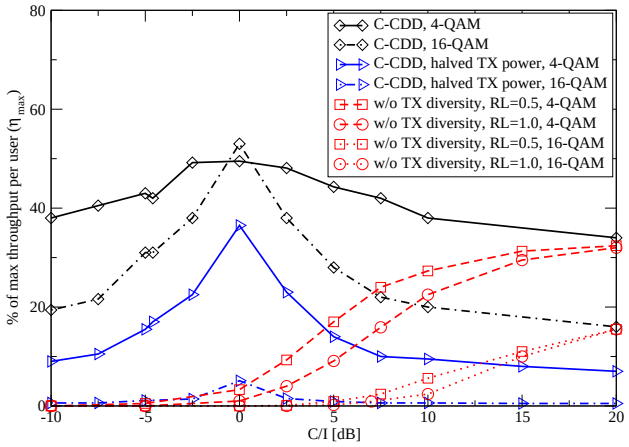

Fig. 11. Throughput per user for 4-QAM and 16-QAM versus C/I using no transmit diversity or C-CDD with full and halved transmit power

modulations.

The C-CDD outperforms the conventional system at the cell border for all scenarios. For 4-QAM and C-CDD, a reliable throughput along the cell border is achieved which is close to its maximum throughput of $\eta_{\max}/2$. Directly at the cell border, the throughput can be increased by using 16-QAM. A power and/or modulation adaptation from the BSs opens the possibility for the MT to request a higher throughput in the critical cell border area.

The simulation results above have shown that C-CDD is capable to improve the performance at the cell borders of a cellular mobile radio communications system. The improvement itself results from an increased degree of diversity, which is achieved through the reception of data signals from more than one BS. This multi-BS signal transmission works well especially at the cell borders because the received signal power levels are balanced. On the other hand, if the mobile is located in the inner part of a cell, the received signal power is severely unbalanced due to propagation loss. This reduces the influence of C-CDD drastically. Therefore, it is desirable to use C-CDD or C-DD in the outer part of the cells, depending on available resources in adjacent cells. It is possible to apply C-CDD or C-DD to three neighboring BSs or sectorized adjacent cells. All these characteristics can be also utilized by soft handoff concepts.

V. Summary

In this paper, we have briefly introduced the concept of cyclic delay diversity (CDD). Compared to classical MIMO techniques, like Space-Time coding, CDD provides the advantage of standard compatibility. This means that a standard receiver does not need to be changed, when implementing CDD in addition. Therefore, no additional computational effort is necessary at the receiver side.

Due to standard compatibility, the effect of CDD at the receiver is observable only by modified channel propagation conditions. We have analyzed CDD in terms of its influence to the channel properties such as the effective channel transfer function and the subcarrier fading correlation. We have seen that the effective subcarrier correlation function is factorizable into a factor depending on the propagation properties itself and into another one, which depends solely on the CDD antenna configuration. This allows a systematic design of independent fading processes for specific sets of subcarriers, which can be used to optimize diversity and coding gain exploited by channel- or spreading-codes.

We have further applied the CDD principle to DVB-T, which is an OFDM based broadcasting systems, and to an OFDMA based proposal for a cellular mobile radio communications system of the 4^{th} generation. The application to cellular systems has led to a variant of CDD which is called cellular cyclic delay diversity (C-CDD), since the different TX-antenna CDD signals are transmitted from different base stations (cells).

Both applications have been investigated by simulations. For DVB-T we have seen significant performance gains in form of SNR gains especially for the indoor propagation scenario, which inherently provides less diversity compared to the considered outdoor propagation channel. By applying C-CDD the performance of a cellular mobile radio communications system increases drastically when the mobile terminal is located at the cell border, which is usually the critical scenario.

Acknowledgments

Parts of this work have been performed in the framework of the IST projects WINNER II (FP6-2004-IST-4-027756) and PLUTO (FP6-2004-IST-4-026902), which are partly funded by the European Union.

References

[1] V. Tarokh, N. Seshadri, and A. R. Calderbank, “Space-time codes for high data rate wireless communication: Performance criterion and code construction,” *IEEE Transactions on Information Theory*, vol. 44, no. 2, pp. 744–764, Mar. 1998.

[2] S. M. Alamouti, “A simple transmit diversity technique for wireless communications,” *IEEE Journal on Selected Areas in Communications*, vol. 16, no. 8, pp. 1451–1458, Oct. 1998.

[3] A. Hiroike, F. Adachi, and N. Nakajima, “Combined effects of phase sweeping transmitter diversity and channel coding,” *IEEE Transactions on Vehicular Technology*, vol. 41, no. 2, pp. 170–176, May 1992.

[4] A. Wittneben, “A new bandwidth efficient transmit antenna modulation diversity scheme for linear digital modulation,” in *Proceedings IEEE International Conference on Communications (ICC 1993), Geneva, Switzerland*, May 1993, pp. 1630–1634.

[5] A. Dammann and S. Kaiser, “Performance of low complex antenna diversity techniques for mobile OFDM systems,” in *Proceedings* 3^{rd} *International Workshop on Multi-Carrier Spread-Spectrum & Related Topics (MC-SS 2001), Oberpfaffenhofen, Germany*, Sept. 2001, pp. 53–64, ISBN 0-7923-7653-6.

[6] ——, “Standard conformable antenna diversity techniques for OFDM and its application to the DVB-T system,” in *Proceedings IEEE Global Telecommunications Conference (GLOBECOM 2001), San Antonio, TX, USA*, Nov. 2001, pp. 3100–3105.

[7] ——, “Transmit/receive antenna diversity techniques for OFDM systems,” *European Transactions on Telecommunications*, vol. 13, no. 5, pp. 531–538, Sept.–Oct. 2002.

[8] A. Dammann, “On antenna diversity techniques for OFDM systems,” Ph.D. dissertation, Universität Ulm, Germany, June 2006, VDI Verlag Düsseldorf, Series 10, No. 766, ISBN 3-18-376610-8.

[9] *Digital Video Broadcasting (DVB); Framing structure, channel coding and modulation for digital terrestrial television*, European Telecommunications Standard Institute (ETSI), July 1999, EN 300 744 V1.2.1.

[10] *Final Report on RF Channel Characterization*, Joint Technical Committee on Wireless Access, Sept. 1993, JTC(AIR)/93.09.23-238R2.

[11] IEEE 802.11-03/940r2, “IEEE P802.11 wireless LANs, TGn channel models,” January 2004.

[12] IST-2003-507581 WINNER, “Final report on identified RI key technologies, system concept, and their assessment,” December 2005.

[13] G. Bauch and J. S. Malik, “Cyclic delay diversity with bit-interleaved coded modulation in orthogonal frequency division multiple access,” *IEEE Transactions on Wireless Communications*, vol. 5, no. 8, pp. 1–9, Aug. 2006.

View publication stats